

Cite this: *RSC Adv.*, 2018, 8, 4478

# Nano metal oxides as efficient catalysts for selective synthesis of 1-methoxy-2-propanol from methanol and propylene oxide†

Jiawei Zhang, Qinghai Cai, \* Jingxiang Zhao and Shuying Zang\*

Nano metal oxides such as  $\text{Fe}_2\text{O}_3$ ,  $\text{Fe}_3\text{O}_4$ ,  $\text{CuO}$ ,  $\text{NiO}$ ,  $\text{ZnO}$  and  $\text{SnO}_2$  were prepared and characterized using XRD, SEM and TEM analysis. These as-prepared metal oxide materials were used as catalysts for the etherification of methanol with propylene oxide (PO). The results showed that  $\alpha\text{-Fe}_2\text{O}_3$  exhibited outstanding catalytic performance with 97.7% conversion and 83.0% selectivity to MP-2 at 160 °C for 8 h. Furthermore, the relationship between the catalytic activity or selectivity and surface basicity or energy gap was investigated. This catalyst could be easily recovered and reused due to its heterogeneous catalytic nature.

Received 7th December 2017  
Accepted 10th January 2018

DOI: 10.1039/c7ra13119d

rsc.li/rsc-advances

## Introduction

Glycol ethers are considered to be important chemicals that combine the best solvency features of alcohols and ethers for synthesizing organic compounds.<sup>1</sup> They are widely used as industrial solvents for coating materials, printing ink, dyeing leather *etc.* Due to the low toxicity of propylene glycol ether, it is expected to be a safe substitute for toxic ethylene glycol ether. Although there are several methods for synthesizing propylene glycol ether, the propylene oxide route is the most convenient and industrially feasible in terms of atom-economy and energy-efficiency. In this method, the epoxide ring of propylene oxide may open at the C–O bond and react with alcohols to form propylene glycol ether, catalyzed by acid or base catalysts. These catalysts include earlier homogeneous acids or bases, such as NaOH, alcoholic sodium,  $\text{H}_2\text{SO}_4$  and  $\text{BF}_3$  *etc.*,<sup>2,3</sup> and later solid acids or bases, *e.g.* acidic zeolites,<sup>4</sup> Mg/Al hydrotalcite,<sup>5</sup> Zn–Mg–Al oxides,<sup>1</sup>  $\text{MgO}$ <sup>6</sup> and amine-modified porous silica<sup>7</sup> *etc.* Very recently, brucite-layer materials,<sup>8</sup>  $\text{Al}_2\text{O}_3/\text{MgO}$ ,<sup>9</sup> and basic and acidic ionic liquids<sup>10,11</sup> have been developed as highly efficient catalysts for the selective synthesis of propylene glycol ether. Because there is much research interest in developing environmentally benign catalysis, we wish to report the preparation of nano metal oxides using a simple method, and highlight their catalytic performance for the synthesis of 1-methoxymethane-2-propanol (MP-2) *via* an atom-economic

reaction. The simply prepared  $\text{Fe}_2\text{O}_3$  catalyst, which is inexpensive and environmentally benign, demonstrated excellent catalytic performance for the synthesis of MP-2. The results are disclosed herein.

## Experimental

### Preparation of the catalysts

Iron oxide was prepared using the following procedure.<sup>12</sup> 30 mL of  $\text{FeCl}_3$  aqueous solution ( $1 \text{ mol L}^{-1}$ ), 2.5 g of urea and 2 mL of polyethylene glycol (PEG-400) as a dispersant were added to a three-necked flask fitted with a reflux condenser and an electric heater. Ammonia solution (28%) was added dropwise to the mixed solution to maintain a pH of 3.7 to afford  $\text{Fe}(\text{OH})_3$ . Thereafter, the reactor was heated to 80 °C and aged at this temperature for 8 h. The mixed solution was then ultrasonically treated at room temperature for 20 min, followed by filtration to remove the filtrate. The obtained solid was washed with deionized water and anhydrous ethanol. Thereafter, it was dried at 100 °C for 12 h, and then calcined at 500 °C for 2 h in a muffle furnace to afford nano-iron oxide. Other oxides, such as  $\text{CuO}$ ,  $\text{ZnO}$ ,  $\text{NiO}$  and  $\text{SnO}_2$ , were prepared with the same method to that of iron oxide, using  $\text{CuSO}_4$ ,  $\text{ZnSO}_4$ ,  $\text{NiCl}$  and  $\text{SnCl}_4$  aqueous solutions as precursors. However, the pH values for precipitation of  $\text{Cu}(\text{OH})_2$ ,  $\text{Zn}(\text{OH})_2$ ,  $\text{Ni}(\text{OH})_2$  and  $\text{Sn}(\text{OH})_4$  were adjusted to 4.7, 6.0, 7.2 and 2.5, respectively.  $\text{Fe}_3\text{O}_4$  was prepared according to the literature.<sup>13</sup>

### Catalyst characterization

XRD of the sample was performed on a Bruker-D8 Advance X-ray diffractometer with  $\text{Cu K}_\alpha$  radiation (40 kV and 36 mA). TEM measurements were taken on a JEM-2100 electron microscope (JEOL Japan) with an acceleration voltage of 200 kV. The

Key Lab of Remote Sensing Monitoring of Geographic Environment, College of Heilongjiang Province, School of Chemistry and Chemical Engineering, Harbin Normal University, No. 1 Shida Road Limin development Zone, Harbin 150025, P. R. China. E-mail: Zsy6311@163.com; caiqinghai@yahoo.com; Fax: +86-451-88060580; Tel: +86-451-88060580

† Electronic supplementary information (ESI) available. See DOI: 10.1039/c7ra13119d



morphology of the catalysts was observed using a Hitachi S-4800 scanning electron microscope (SEM).

### Catalytic test and analytic procedure

1.0 mL (14.4 mmol) of propylene oxide, 21 mL (0.52 mol) of methanol and 0.1 g of iron oxide catalyst were added, in turn, into a stainless steel 100 mL autoclave with a magnetic stirrer in an electric heater. The reactor was heated to 160 °C with fast stirring and the reaction was carried out at this temperature for 8 h. When the reaction was complete, the mixture was filtered to remove the catalyst and the filtrate was analyzed using GC (Agilent 7820) with a FID detector equipped with HP-5, a 30 m × 0.32 mm × 0.25 μm column and GC-MS (Agilent GC 7890A-5975C).

## Results and discussion

### Characterization of the catalysts

Fig. 1 presents the XRD pattern of the prepared iron oxide sample recorded in the  $2\theta$  range of 10–90°. It can be seen from the figure that typical diffraction peaks at  $2\theta$  values of 24.1, 33.2, 35.6, 41.0, 49.5, 54.2, 57.7, 62.4 and 64.0° correspond to the diffractions of the (012), (104), (110), (113), (024), (116), (018), (214) and (300) planes, respectively. The intense peaks of the XRD pattern indicate that the  $\text{Fe}_2\text{O}_3$  product was well crystallized and no impurity diffraction peaks were observed, implying that almost single phase  $\text{Fe}_2\text{O}_3$  was successfully prepared. All diffraction peaks were perfectly indexed, which was in agreement with the data of  $\alpha\text{-Fe}_2\text{O}_3$  (hematite, JCPDS 33-0664). Moreover, the average crystallite size of the product was estimated to be 31.7 nm using the Debye–Scherrer equation. The XRD patterns of the other metal oxides, such as CuO, NiO, ZnO,  $\text{SnO}_2$  and  $\text{Fe}_3\text{O}_4$ , are shown in Fig. SI1–5.†

**SEM and TEM.** Fig. 2 shows the scanning electron microscopy (SEM) image of the  $\text{Fe}_2\text{O}_3$  sample. As seen from the figure, iron oxide particles of about 30 nm in size were well dispersed and their sizes were in agreement with the value calculated using the Debye–Scherrer equation. In addition, the transmission electron microscopy (TEM) image of the  $\text{Fe}_2\text{O}_3$  sample

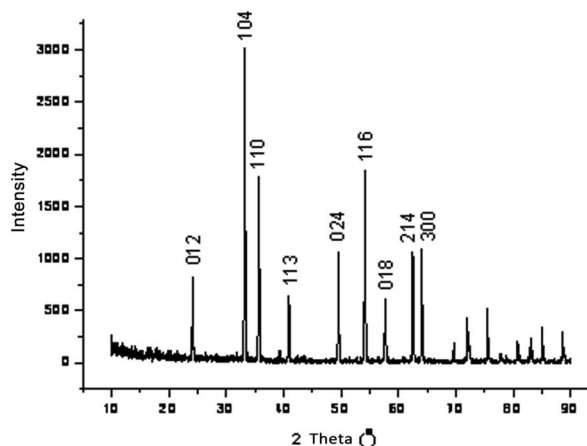


Fig. 1 XRD pattern of  $\text{Fe}_2\text{O}_3$ .

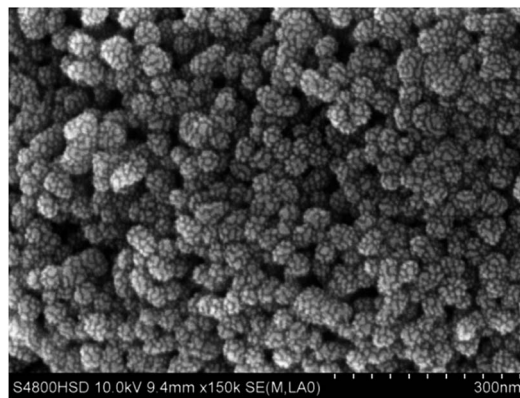


Fig. 2 SEM image of iron oxide sample.

also showed the same result as the SEM of  $\text{Fe}_2\text{O}_3$ . Nano-particles of about 30 nm in size are shown in Fig. 3. The SEM and/or TEM images of other metal oxides, such as CuO, NiO, ZnO,  $\text{SnO}_2$  and  $\text{Fe}_3\text{O}_4$  (TEM), are shown in Fig. SI6–10.† The morphologies of these oxides can also be seen in Fig. SI6–10:† particles of about 20 nm for  $\text{Fe}_3\text{O}_4$ , particles of 200–300 nm for CuO, particles of about 100 nm for ZnO, and aggregations composed of ~30 nm sized particles for  $\text{SnO}_2$  and NiO.

**Catalytic activity.** The catalytic activity of  $\alpha\text{-Fe}_2\text{O}_3$  and the other metal oxides such as  $\text{Fe}_3\text{O}_4$ , CuO, NiO, ZnO and  $\text{SnO}_2$  for the etherification of methanol with propylene oxide (PO) was assessed. The results are summarized in Table 1. The data show that the  $\alpha\text{-Fe}_2\text{O}_3$  catalyst possessed very high activity for etherification with a conversion of 97.7% and 83.0% selectivity to 1-methoxy-2-propanol (MP-2) at 160 °C for 8 h, corresponding to a TON (turnover number, converted moles per mole catalyst) of 11.5 mol  $\text{mol}_{\text{Fe}}^{-1}$  (entry 1). Also, the CuO catalyst displayed the same activity as  $\alpha\text{-Fe}_2\text{O}_3$ , with a conversion of 97.9% (entry 2), but the selectivity to MP-2 was relatively low with a MP-2/MP-1 (2-methoxy-1-propanol) ratio of only 1.17. Although  $\text{Fe}_3\text{O}_4$  and NiO had a higher MP-2/MP-1 ratio, their catalytic activities for the etherification were lower (entry 3 and 4), exhibiting 26.5 and 56.3% conversions with TONs of 3.0 mol  $\text{mol}_{\text{Fe}}^{-1}$  and 6.1 mol

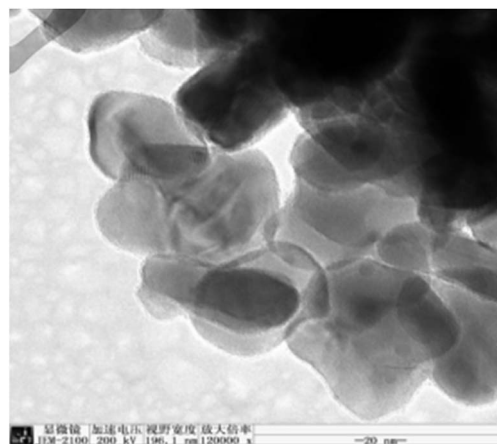


Fig. 3 TEM image of the iron oxide sample.



Table 1 Catalytic activity of some metal oxides<sup>a</sup>

Entry	Oxides	Conv. (%)	Sel. (%)	TON	Rat.	$E_g^{14}$	Bas. <sup>14</sup>
1	$\alpha$ -Fe <sub>2</sub> O <sub>3</sub>	97.7	83.0	11.5	4.88	2.00	1.008
2	CuO	97.9	54.0	11.5	1.17	1.95	0.991
3	Fe <sub>3</sub> O <sub>4</sub>	26.5	80.4	3.0	4.10	—	—
4	NiO	56.3	80.5	6.1	4.13	3.80	0.997
5	ZnO	65.9	59.3	7.7	1.46	3.40	1.001
6	SnO <sub>2</sub>	59.7	59.0	13.0	1.44	3.80	0.927

<sup>a</sup> Reaction conditions: reaction temperature = 160 °C, time = 8 h, catalyst = 0.1 g, molar ratio of methanol to PO = 36 : 1; Conv. = conversion, Sel. = selectivity to MP-2, TON = turn over number (mol mol<sub>M</sub><sup>-1</sup>, M = Fe, Cu, Ni, Zn and Sn), rat. = ratio of MP-2/MP-1,  $E_g$  = energy gap, Bas. = basicity.

mol<sub>Ni</sub><sup>-1</sup>, respectively. Similarly, ZnO and SnO<sub>2</sub> presented almost the same conversions and selectivities to MP-2 (entry 5 and 6). The difference in the catalytic activity of these metal oxides was not directly related to their particle size (Fig. S16–10†), but was instead related to their acid–base properties on the surface.<sup>1</sup> Compared with the reported works in the literature,  $\alpha$ -Fe<sub>2</sub>O<sub>3</sub> exhibited higher activity, although the catalysts Mg, Al-LDH and Zn, Mg, Al-LDH displayed high conversions of 92.4% or 95.9% and 96.5% or 90.9% of selectivity to MP-2, achieving TONs of 12.8 and 16.7,<sup>1,5</sup> respectively. However, the preparation process for these catalysts was more complicated than that of  $\alpha$ -Fe<sub>2</sub>O<sub>3</sub>.

It has been previously reported that in  $\alpha$ -Fe<sub>2</sub>O<sub>3</sub>, oxide ions (O<sup>2-</sup>) are arranged along the plane of a hexagonal closed-packed lattice, whereas two-thirds of the octahedral interstices are occupied by Fe<sup>3+</sup> cations in the basal plane.<sup>15</sup> Acid–base ion pairs (O<sup>2-</sup>–Fe<sup>3+</sup>) are inevitably formed on the surface of  $\alpha$ -Fe<sub>2</sub>O<sub>3</sub>, and play an important role the addition reaction. The acidic sites (Fe<sup>3+</sup>) are responsible for PO conversion, and the basic sites (O<sup>2-</sup>) are beneficial for generating MP-2,<sup>11</sup> which is confirmed by the basicity order list in Table 1. Furthermore, the catalytic activity of the metal oxides is related to their energy gap,<sup>14</sup> that is, the lower the energy gap, the higher the activity of these metal oxides, because it is easier for electrons to transition when the energy gap is low, enhancing the formation of acid–basic sites on the surface. On the other hand,  $\alpha$ -Fe<sub>2</sub>O<sub>3</sub> catalysts usually possess redox properties for catalyzing organic synthesis reactions, such as oxidation of toluene, benzylation of benzene and other aromatics *etc.*<sup>16,17</sup> The redox species in the reaction systems are advantageous for the ring opening reaction of PO.<sup>18</sup> Therefore, the excellent catalytic performance of the  $\alpha$ -Fe<sub>2</sub>O<sub>3</sub> catalyst compared with the other metal oxides was ascribed to the surface properties.

### Effect of reaction conditions

Using  $\alpha$ -Fe<sub>2</sub>O<sub>3</sub> as the catalyst, the effect of reaction time on the catalytic activity was investigated. As shown in Fig. 4, the conversion of PO increased as the reaction proceeded from 3 to 8 h at 110 °C. The conversion approached to 57.6% as the reaction was carried out for 8 h. Then, the conversion slightly increased as the reaction time was prolonged to 9 h, implying

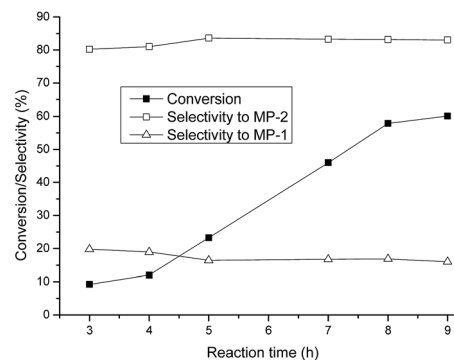


Fig. 4 Dependence of reactivity on the reaction time. Reaction conditions: temperature = 110 °C, catalyst = 0.1 g, molar ratio of methanol to PO = 36 : 1.

that the thermodynamic equilibrium of the reaction was almost achieved at that time. Furthermore, the selectivity to MP-2 increased as the time was prolonged from 3 to 5 h, while on the contrary, the selectivity to MP-1 was decreased over this range. The selectivity to MP-2, as well as MP-1, was almost constant during the reaction time from 5 to 9 h.

As the reaction temperature was raised, the conversion rapidly increased to a maximum at 160 °C, and basically remained unchanged at 170 °C (Fig. 5). The change in the conversion with temperature was probably due to the control of the reaction kinetics, that is, high temperature can accelerate the reaction rate and shorten the time needed to reach equilibrium. Thus, increasing the reaction temperature is greatly advantageous to forming the product. Unexpectedly, the selectivity to MP-2 was independent of the reaction temperature in the range from 110 to 190 °C, retaining the value at 83.0% over the whole temperature range. This is rare in the catalytic synthesis of organic compounds.

### Reactivity of other alcohols

Other alcohols such as ethanol, propanol, butanol, iso-butanol, amyl alcohol, iso-amyl alcohol and octanol were then applied as alternatives to methanol, and the etherification reactions of PO

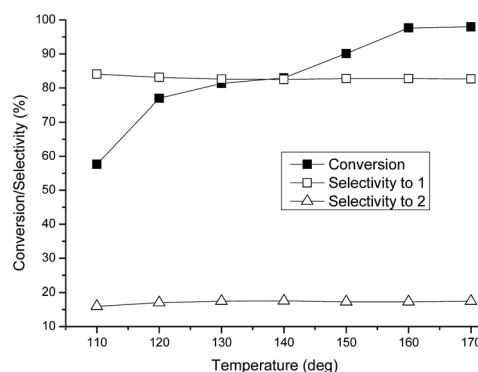


Fig. 5 Dependence of reactivity on the reaction temperature. Reaction conditions: reaction time = 8 h, catalyst = 0.1 g, molar ratio of methanol to PO = 36 : 1.



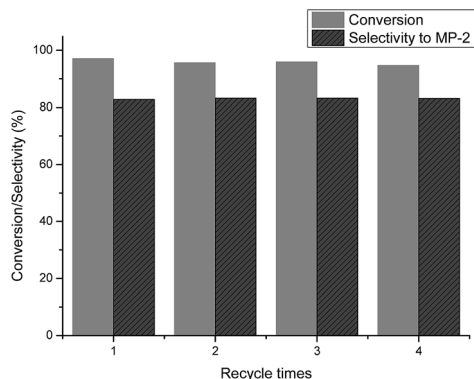


Fig. 6 The reusability of the catalyst.

with these alcohols were also examined in the presence of  $\alpha$ - $\text{Fe}_2\text{O}_3$  as a catalyst under the same conditions (Table 2). As shown in the table, the reactivity was reduced as the length of the carbon chain in the alcohols increased (entry 1–8), so that octanol exhibited very low reactivity for this reaction with 31.6% conversion (entry 8). By comparison, the lower reactivity of iso-butanol and iso-amyl alcohol compared to that of butanol and amyl alcohol is related to the steric effect of secondary alcohols (entry 4–7). Furthermore, the selectivity to 1-alkoxy-2-alcohol was also lower than that of the methanol system, with 48.0 to 64.2% selectivity achieved.

Table 2 Reactivity of other alcohols with PO

Entry	Alcohols	Conv. (%)	Sel. to MP-2 (%)
1	Methanol	97.7	82.6
2	Ethanol	69.8	50.9
3	Propanol	64.7	49.6
4	Butanol	63.9	64.2
5	Iso-butanol	50.2	52.1
6	Amyl alcohol	51.6	50.0
7	Iso-amyl alcohol	41.6	48.0
8	Octanol	31.6	50.0

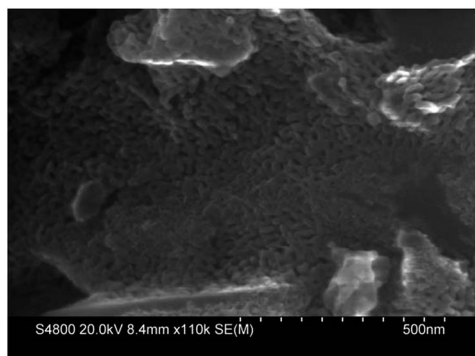


Fig. 7 SEM image of the used catalyst.

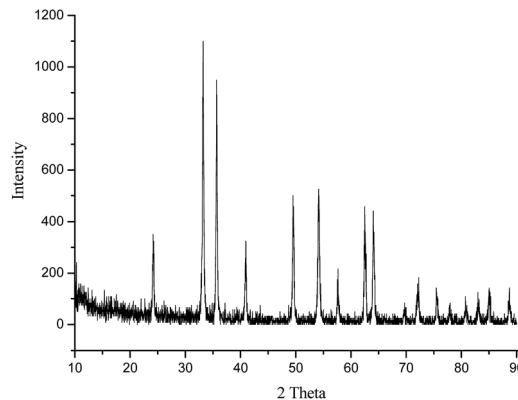


Fig. 8 XRD pattern of the catalyst after being used four times.

### The stability of the catalyst

In order to further evaluate the performance of the  $\alpha$ - $\text{Fe}_2\text{O}_3$  catalyst, reuse tests of  $\alpha$ - $\text{Fe}_2\text{O}_3$  were conducted. The catalyst was separated by filtration after the first test, and then reused for the next run under the same conditions. The results are depicted in Fig. 6.

As shown in the figure, the catalytic activity of the reused catalyst was almost unaffected even at the fourth run, exhibiting >95.0% conversion and retaining 83.0% selectivity to MP-2. The SEM image of the reused catalyst is shown in Fig. 7. Aggregation of the  $\text{Fe}_2\text{O}_3$  nanoparticles was observed when they were reused four times, but their phase composition did not change, as shown in the XRD pattern of the used  $\text{Fe}_2\text{O}_3$  catalyst (Fig. 8). These results imply that the catalyst can be efficiently recovered and recycled.

## Conclusions

Nano metal oxide materials were prepared and characterized using XRD, SEM and TEM analysis. These oxides were used for the etherification of methanol with propylene oxide (PO) to form 1-methoxy-2-propanol (MP-2). The as-prepared  $\text{Fe}_2\text{O}_3$  material, recognized as  $\alpha$ - $\text{Fe}_2\text{O}_3$ , was found to be an effective catalyst for the etherification of methanol with propylene oxide (PO), with 97.7% conversion and 83.0% selectivity to MP-2 at 160 °C for 8 h, and achieving a TON of 11.5 mol mol $_{\text{Fe}}^{-1}$ . The high catalytic activity and selectivity to MP-2 of this catalyst, which was prepared using a simple method, can be attributed to its low energy gap and high basicity. This catalyst can be easily recovered and reused due to its heterogeneous catalytic nature. Thus, the simply prepared and environmentally benign  $\alpha$ - $\text{Fe}_2\text{O}_3$  catalyst demonstrates great potential for application in industry.

## Conflicts of interest

There are no conflicts to declare.

## Acknowledgements

We make a great acknowledgement for the financial support of this work from the National Natural Science Foundation of



China (No. 21671050, 41571199), the Natural Science Foundation of Heilongjiang Province (No. 2015003, B201119) and the Foundation for academic leaders of Harbin (No. 2013RFXXJ009).

## Notes and references

- 1 W. Cheng, W. Wang, Y. Zhao, L. Liu, J. Yang and M. He, *Appl. Clay Sci.*, 2008, **42**, 111.
- 2 H. A. Pecorini and J. T. Banchemo, *Ind. Eng. Chem.*, 1956, **48**, 1287.
- 3 H. C. Chitwood and B. T. Freurec, *J. Am. Chem. Soc.*, 1948, **68**, 680.
- 4 W. Y. Zhang, H. Wang, Q. B. Li, Q. N. Dong, N. Zhao and W. Wei, *Appl. Catal., A*, 2005, **294**, 188.
- 5 H. Y. Zeng, Y. J. Wang, Z. Feng, K. Y. You, C. Zhao, J. W. Sun and P. L. Liu, *Catal. Lett.*, 2010, **137**, 94.
- 6 W. Y. Zhang, H. Wang, W. Wei and Y. H. Sun, *J. Mol. Catal. A: Chem.*, 2005, **231**, 83.
- 7 X. Zhang, W. Zhang, J. Li, N. Zhao, W. We and Y. H. Sun, *Catal. Commun.*, 2007, **8**, 437.
- 8 M. N. Timofeeva, A. E. Kapustin, V. N. Panchenko, E. O. Butenko, V. V. Krupskaya, A. Gil and M. A. Vicente, *J. Mol. Catal. A: Chem.*, 2016, **423**, 22.
- 9 Y. Zhang, B. Lu, X. Wang, J. Zhao and Q. Cai, *Appl. Catal., A*, 2011, **408**, 125.
- 10 C. Y. De, Q. H. Cai, X. G. Wang, J. X. Zhao and B. Lu, *J. Chem. Technol. Biotechnol.*, 2011, **86**, 105.
- 11 Y. Bai, Q. Cai, X. Wang and B. Lu, *Kinet. Catal.*, 2011, **52**, 396.
- 12 H. Tang, H. Wang, B. Lu, J. Zhao and Q. Cai, *Mol. Catal.*, 2017, **431**, 27.
- 13 W. Zhang, B. Lu, H. Tang, J. Zhao and Q. Cai, *J. Magn. Magn. Mater.*, 2015, **381**, 401.
- 14 R. R. Reddy, Y. N. Ahammed, P. A. Azeem, K. R. Gopal and T. V. R. Rao, *J. Non-Cryst. Solids*, 2001, **286**, 169.
- 15 M. Mishra and D.-M. Chun, *Appl. Catal., A*, 2015, **498**, 126.
- 16 X. Li, X. You, B. Lu, X. Wu, J. Zhao and Q. Cai, *Ind. Eng. Chem. Res.*, 2014, **53**, 20085.
- 17 S. Fan, Y. Pan, H. Wang, B. Lu, J. Zhao and Q. Cai, *Mol. Catal.*, 2017, **442**, 20.
- 18 Y. Ogata, Y. Sawaki and H. Shimizu, *J. Org. Chem.*, 1978, **43**, 1760.

